International Journal of New Horizons in Physics

http://dx.doi.org/10.12785/ijnhp/040202

α -Cluster optical potential model of pions scattering from ^{28}Si

M. El-Azab Farid [1], *A. A. Ebrahim*[1], *B. M. Elyan* [2,*], *S. R. Mokhtar*[1], *and M. A. El-Zohry*[2]

[1] Physics Department, Assiut University, Assuit 71516, Egypt
[2] Physics Department, Sohag University, Sohag 82524, Egypt

Received: 23 Mar. 2017, Revised: 18 Jun. 2017, Accepted: 25 Jun. 2017
Published online: 1 Jul. 2017

Abstract: Analysis of $\pi^{\pm}+^{28}Si$ elastic scattering at energies 21.69, 48.9, 130, 180 and 226 MeV and inelastic scattering at energies 130, 180 and 226 MeV leading to the lowest 2^+ and 3^- states of ^{28}Si have been carried out in the framework of the alpha-clustering single folding model. In the elastic scattering analysis, the real part of the considered potential is taken also in the phenomenological Woods-Saxon form besides the alpha-clustering SF model. Our results are compared with the experimental data and gave a good fit. The values of the extracted reaction cross sections in the two cases are similar to each other. The calculated deformations lengths are similar to those estimated from other studies.

Keywords: elastic scattering, inelastic scattering, Pions, alpha-clustering single folding mode

1 Introduction

Many studies have been carried out on the scattering of pions from nuclei. Satchler [1] achieved a great success in presenting a local phenomenological optical potential, of a Woods Saxon form, to analyze the elastic and inelastic scattering of charged pions from $^{40,48}Ca$, ^{58}Ni,^{90}Zr, ^{118}Sn and ^{208}Pb at energies from 100 to 300 MeV. Using the kisslinger local potential [2] for pions elastic and inelastic scattered from different nuclei at different energies also obtain a great success which motivate many researchers to analyze the scattering of pions from nuclei over the last decades.

In the present work we will employ the alpha-clustering single folding model to describe $\pi^{\pm}+^{28}Si$ reaction which is based on the folded form of the pion-nucleus local optical potential and the cluster structure of the target. The real part of the nuclear optical potential is calculated in the framework of the alpha-clustering SF model, while the imaginary part is taken in the phenomenological Woods-Saxon form. The effective pion-alpha interaction is taken in the Gaussian form.

The shape of the binding energy curve reflects the nuclear structure. The concept of alpha clustering results from the phenomena of alpha decaying from nuclei with a tightly bound structure. Even nuclei such as ^{4}He,^{8}Be,^{12}C,^{16}O, etc. have high binding energy and all of these nuclei can be considered to be composed of α -particles. Therefore, nucleus mass number AT equals 4m where m is integral number of α -particles of the nucleus. ^{28}Si is a nucleus consists of seven $\alpha-$particle , each α -particle is bounded more weakly than a nucleon in the ^{28}Si nucleus.

The motivation of our study is the success of the considered model in analyzing elastic and inelastic scattering of charged pions from other nuclei where M. El-Azab Farid and A. A. Ebrahim [4] succeed in studying elastic and inelastic scattering of charged pions in the framework of the considered model from ^{12}C and ^{16}O through a board energy range (100-766 MeV).

The manuscript of this work is ordered as follows: the theoretical formalism is showed in section 2 ,the procedure is explained in section 3, the results and discussion are displayed in section 4, and the conclusion is briefed in section 5.

2 Theoretical formalism

The total pion- nucleus potential (SF case) expressed is expressed as:

$$U(R) = V_{SF}(R) + iW(R) + V_C(R) \qquad (1)$$

* Corresponding author e-mail: basma.elyan@yahoo.com

where R is the projectile-target separation, $V_{SF}(R)$ and $W(R)$ donate the real and imaginary parts of the potential respectively and $V_C(R)$ term is the repulsive Coulomb potential.

Alpha-cluster density function $\rho_c(r')$ relates to nuclear matter density function $\rho_m(r)$ by [5,6]:

$$\rho(r)_m = \int \rho_c(r')\rho_\alpha(\bar{r}-\bar{r'})d\bar{r'} \quad (2)$$

where r,r' and $\rho_\alpha(r)$ are the relative position vector between the nucleons, the position vector of an α -cluster and the matter density of α -particle respectively. $\rho_c(r')$ and $\rho_m(r)$ are expressed in the harmonic oscillator shape as

$$\rho_c(r') = \rho_{0c}(1+\gamma r'^2)\exp(-\xi r'^2) \quad (3)$$

$$\rho_m(r) = \rho_{0m}(1+\omega r^2)\exp(-\beta r^2) \quad (4)$$

and $\rho_\alpha(r)$ can be expressed in the Gaussian form as:

$$\rho_\alpha(r) = \rho_{0\alpha}\exp(-\lambda r^2) \quad (5)$$

where $\rho_{0(c,m,\alpha)}, \gamma, \xi, \omega, \beta$, and λ are constants, and

$$\xi = \frac{\beta\lambda}{\eta}, \eta = \lambda-\beta, \gamma = \frac{2\omega\lambda^2}{\eta(2\eta-3\omega)}, and \rho_{0c} = m(\xi/\pi)^{3/2}[1+3\gamma/2\xi]^{-1} \quad (6)$$

By using the alpha-clustering model to calculate the optical potential through the SFC model, the real part of the optical potential becomes:

$$V_{SF}(R) = \int \rho_c(r')V_{n-\alpha}(\bar{R}-\bar{r'})d\bar{r'} \quad (7)$$

By considering the nucleon-α interaction $V_{n-\alpha}$ in Gaussian form as:

$$V_{n-\alpha}(\bar{R}-\bar{r'}) = -V_0\exp(-k|\bar{R}-\bar{r'}|^2), k = 1/a^2 \quad (8)$$

where a is the range parameters, we obtains:

$$V_{SF}(R) = -(\frac{\pi}{\mu})^{(3/2)}V_0\rho_{0c}\exp(\frac{kR^2}{\mu}(k-\mu))[1+\frac{3\gamma}{2\mu}+\frac{\gamma k^2R^2}{\mu^2}] \quad (9)$$

The inelastic scattering measurements are analyzed using a deformed optical model potential (DP) [13] where the radial dependence of the transition potential is:

$$V_l(R) = -\delta_{real}\frac{dV(R)}{dR} \quad (10)$$

where δ_{real} is the real deformation length that determines the strength of the interaction and $V(R)$ expresses the complex optical potential determined by the measured elastic scattering. And the transition density can be expressed by:

$$\rho_l(r) = -\delta_{real}\frac{d\rho_c(r)}{dr} \quad (11)$$

Table 1: Parameters of the nuclear matter and the alpha cluster densities of ^{28}Si.

ρ_{0m} (fm $^{-3}$)	ω (fm $^{-2}$)	β (fm $^{-2}$)
0.2050	0.1941	0.2112
ρ_{0c} (fm $^{-3}$)	γ (fm $^{-2}$)	η (fm $^{-2}$)
0.0357	0.9745	0.302

The imaginary transition potential is obtained by deriving the imaginary central potential as:

$$W_l(R) = -\delta_{imag}w_0\frac{d}{dR}[1+\exp(\frac{R-r_iA_T^{1/3}}{a_i})]^{-1} \quad (12)$$

where δ_{imag} is the real deformation length. The value of the deformation parameter β is to be adjusted to obtain a reasonable agreement with the experimental data shown in the figures below. Deformation lengths $(\delta_{real}, \delta_{imag})$ are found from the deformation parameter by using the following relations :

$$\delta_{real} = \beta r_V A^{1/3} \quad (13)$$

$$\delta_{imag} = \beta r_W A^{1/3} \quad (14)$$

3 Procedure

We will analyze the pion nucleus elastic and inelastic scattering in the framework of the alpha-clustering SF model which the folding calculations are based on the alpha-cluster of the target nuclei (^{28}Si). The effective pion-alpha interaction is taken in the Gaussian form eq.(8) with range parameters equal to 2.13 fm [4] and the nuclear density is taken in a cluster form with parameters calculated according to eq.(6). The nuclear matter densities parameters [6] and the alpha cluster densities parameters are listed in table 1. The real part of the considered potential (in the elastic scattering calculations) is taken also in the phenomenological Woods-Saxon form [3] besides the alpha-clustering SF model.

The effective bombarding energy E_{eff} and the effective pion mass M_π and values used in the present work are listed in table 2 which are calculated according to the following equations [7]:

$$E_{eff} = M_\pi E_{c.m}/\mu \quad (15)$$

where $E_{c.m}$ is the center of mass kinetic energy and μ is the reduced mass and is defined as:

$$\mu = \frac{M_\pi m_T}{M_\pi + m_T}$$

where m_T is the target mass

$$M_\pi = \gamma_\pi m_\pi, \gamma_\pi = (y+\gamma_L)/(1+y^2+2y\gamma_L)^{1/2} \quad (16)$$

Table 2: Pion kinetic energy E_{lab} and the corresponding effective pion mass μ_π and effective bombarding energy E_{eff} values of ^{28}Si.

E_{lab} (MeV)	E_{eff} (MeV)	μ_π
21.69	20.267	0.17292
48.9	42.704	0.20175
130	99.413	0.28733
180	130.59	0.33983
226	158.01	0.38796

where m_π is the pion mass and equals 0.1499 atomic mass unit and y and γ_L are defined as:

$$y = m_\pi/m_T, \gamma_L = 1 + (E_{lab}/m_\pi c^2)$$

where E_{lab} is the pion bombarding energy in the laboratory system.

In the elastic scattering analysis, the real part of the OMP is calculated by two ways (SFC model and WS form) and the imaginary part is calculated using WS form.

The DOLFIN [8] computer code is used to calculate the real part of the SFC potential that we will inserting it's outputs in (a)-The HIOPTIM-94 [9] computer code to calculate the angular distributions of the elastic scattering differential cross sections . (b)- The DWUCK4 [14] computer code with the calculated imaginary part parameters W,$r_w$and a_w (which is take from HIOPTIM-94 outputs) to calculate the angular distributions of the inelastic scattering differential cross sections Then we will compare the obtained theoretical data with the experimental one.

We varied more than one parameter to obtain a reasonable fits with the experimental data and all parameters used in calculations are listed in tables below.

In our calculations we considered uniform errors 10% for all experimental data in order to minimize the chi-square value χ^2 which is defined as:

$$\chi^2 = \frac{1}{N}\sum_{i=1}^{N}[\frac{\sigma_{cal}(\theta_i) - \sigma_{exp}(\theta_i)}{\Delta\sigma_{exp}(\theta_i)}]^2 \qquad (17)$$

where N is the number of differential cross section data points, $\sigma_{cal}(\theta_i)$ is the ith calculated cross section, $\sigma_{exp}(\theta_i)$ and $\Delta\sigma_{exp}(\theta_i)$are the corresponding experimental cross section and its relative uncertainty, respectively.

4 Results and discussion

4.1 $\pi^\pm + ^{28}Si$ elstic scattering

We will study the differential cross section of the elastic scattering of $\pi^\pm$ from ^{28}Si at energies 21.69, 48.9, 130, 180, and 226 MeV. The best fit depth V_0 values for the considered energies is showing in figure 1 where we considered it as a free parameter in our calculations. From this figure we notice that the depth for (π^+, π^-) from ^{28}Si is energy dependent. The depth for $\pi^+ + ^{28}Si$ reaction increases from 7.025 MeV to 43.4 MeV as the energy increases from 21.69 MeV to 130 MeV then decreases to 33.875 MeV at energy 180 MeV and grows up again to reach 41.75 MeV at energy 226 MeV and for $\pi^- + ^{28}Si$ reaction increases from 5.95 MeV to 40.325 MeV as the energy increases from 21.69 MeV to 130 MeV then decreases to 17.375 MeV at energy 180 MeV and grows up again to reach 24.75 MeV at energy 226 MeV. This behavior is referred to the resonance energy ($\sim$ 200 MeV), a strong absorption resulted from the resonance character of the pion-nucleon amplitude is dominant in the pion-nucleus scattering [4].

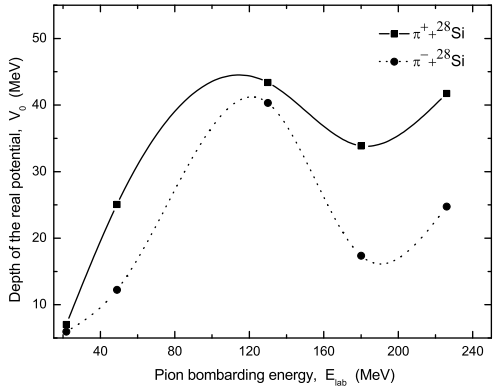

Fig. 1: The energy dependence of the potential depth used in the SF calculations.

21.69, 48.9, 130, 180 and 226 MeV for (π^+, π^-) from ^{28}Si are shown in figs. 2 and 3. It can be seen from these figures that our results gives a considerable agreement at all considered energies with experimental data [10,12] and predict well maxima and minima positions, in both cases of using SF model or Woods-Saxon form except a small shift in maxima at energy 226 MeV for the reaction $\pi^+ + ^{28}Si$. The agreement with experimental data is excellent in both cases at energies 21.69, 48.9 MeV. There is an overestimation at larger angles with energies 130 and 180 MeV.

The best fit SF model and Woods-Saxon optical potential parameters for $\pi^\pm$ scattering from ^{28}Si are listed in tables 3, 4 and 5. The imaginary part parameters (W, r_w, a_w) have the same values in the two cases. scattering of π^+ scattering from ^{28}Si.

The optical model calculations in two cases (SFC model and WS form) give reaction cross sections σ_R, as listed in tables 3, 4 and 5 and shown in figs. 4 and 5. We can see form these figures that the reaction cross section

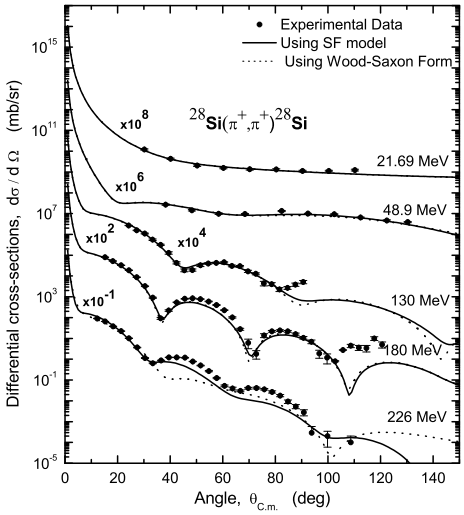

Fig. 2: The angular distributions of the elastic differential cross sections for π^+ scattered from ^{28}Si calculated by SF model (solid curves) and by Wood-Saxon form (dotted curves)

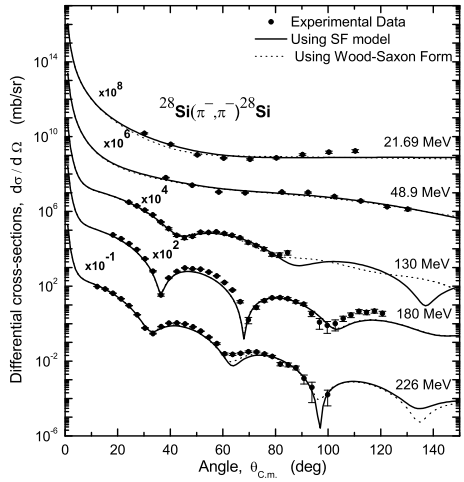

Fig. 3: As in fig. 2 but for π^- scattered from ^{28}Si.

strongly depends on energy and its values in the two cases are so close at all considered energies.

Table 3: Best fit SF model parameters for the elastic scattering of π^+ scattering from ^{28}Si; E_{lab} (MeV), V_0 (MeV), W (MeV), r_W (fm), a_W (fm), and σ_R (mb).

E_{lab}	V_0	W	r_W	a_W	χ^2/N	σ_R
21.69	7.025	175.344	0.6078	0.242	2.815	248.5
48.9	25.05	970	0.4784	0.19	2.489	224.4
130	43.4	72.902	1.0402	0.7818	11.09	767.8
180	33.875	74.033	1.145	0.65	28.09	717.9
226	41.75	73.496	1.0058	0.73	29.01	651.6

Table 4: As in table 3 but for π^- scattered from ^{28}Si; E_{lab} (MeV), V_0 (MeV), W (MeV), r_w (fm), a_w (fm), and σ_R (mb).

E_{lab}	V_0	W	r_w	a_w	χ^2/N	σ_R
21.69	5.95	745.006	0.336	0.2739	14.35	270.8
48.9	12.25	105.104	0.6358	0.156	6.547	240.9
130	40.325	126.035	1.0023	0.664	4.56	810.5
180	17.375	66.07	1.2244	0.58	21.52	726.6
226	24.75	175.18	0.8961	0.65	10.78	692.6

Table 5: Woods-Saxon optical potential parameters for π scattering from ^{28}Si. The imaginary part parameters (W (MeV), r_w (fm), a_w (fm), and σ_R (mb)) have the same values are in tables 3 and 4.

E_{lab}	V	r_v	a_v	χ^2/N	σ_R
		π^+			
21.69	13.05	1.0071	0.803	2.844	249.7
48.9	55.371	0.902	0.8789	4.07	228.5
130	70.193	1.0366	0.8694	11.83	766.4
180	50.686	1.095	0.799	29.34	717.1
226	145.484	0.615	0.411	35.07	608.2
		π^-			
21.69	12.623	0.82	0.559	14.64	260.2
48.9	25	0.8922	0.84	7.191	240.7
130	33.316	1.4029	0.55	4.36	811.4
180	25.662	1.11	0.799	22.34	726.8
226	51.245	1.0103	0.7902	8.926	695.8

4.2 $\pi^{\pm}$ +^{28} Si inelstic scattering

Figures 6, 7, 8 and 9 display the differential cross sections compared with the experimental data [12] of $\pi^{\pm}$ by ^{28}Si $(2^+;1.78MeV)$ and $(3^-;6.88MeV)$ at 130, 180, 226 MeV pion kinetic energies. There is a reasonable agreement with the experimental data [12] except small shifts is some positions.

In figure 6, there is a small shift in the first minimum at 130 and 180 MeV. The resulted data at 226 MeV and the corresponding experimental data have the same behavior with a little shift in values.

In figure 7, there is a small shift in the first minimum at 180 MeV and in the first and the second minima at 226 MeV.

In figure 8, there is an overestimation at large angles $(\theta > 65^o)$ at 130 MeV and at small angles $(\theta < 54^o)$ at

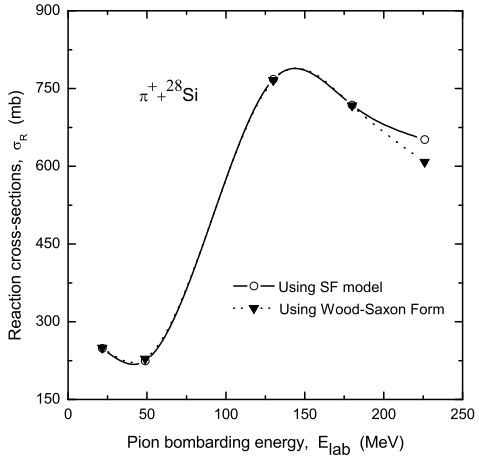

Fig. 4: The energy dependence of reaction cross section for $\pi^{\pm}$ scattered from ^{28}Si calculated by SF model (solid curves) and by Wood-Saxon form (dotted curves).

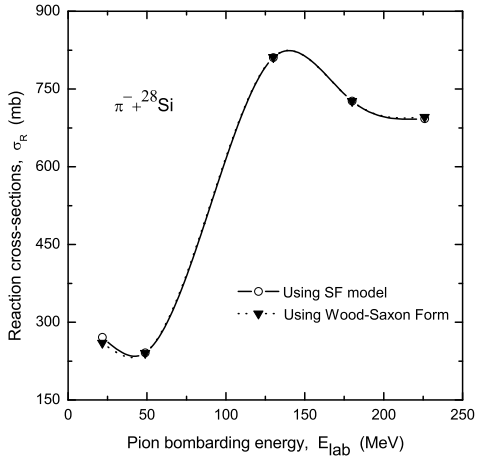

Fig. 5: As in fig.4 but for π^- scattered from ^{28}Si.

226 MeV and a small shift in the first and the second minima at 180 MeV.

In figure 9, there is an overestimation at large angles $(\theta > 55^o)$ at 130 MeV and a small shift in the first and the second minima at 180 and 226 MeV.

Tables 6 and 7 display the resulted values of the deformation parameters β (compared to the values of another study) and the deformation lengths $(\delta_{real}, \delta_{imag})$ according to equations (10) and (11).

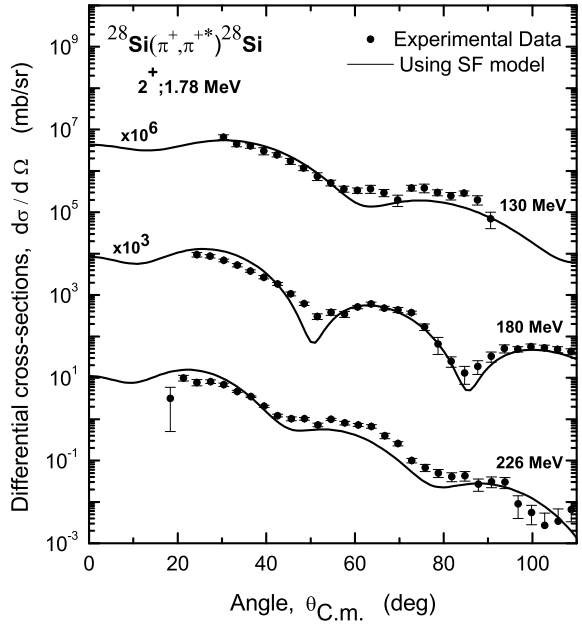

Fig. 6: The angular distributions of the inelastic differential cross sections for π^+ exciting the 2^+ state of ^{28}Si calculated by SF model (solid curves) compared with the experimental data from [12].

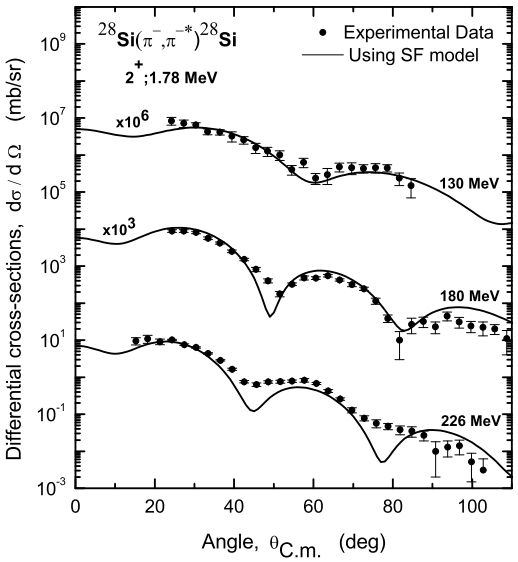

Fig. 7: As in fig.6 but for π^- scattered from ^{28}Si.

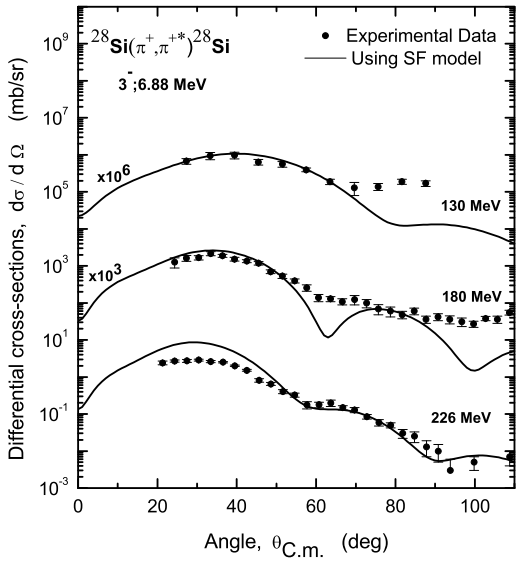

Fig. 8: The angular distributions of the inelastic differential cross sections for π^+ exciting the 3^- state of ^{28}Si calculated by SF model (solid curves) compared with the experimental data from [12]

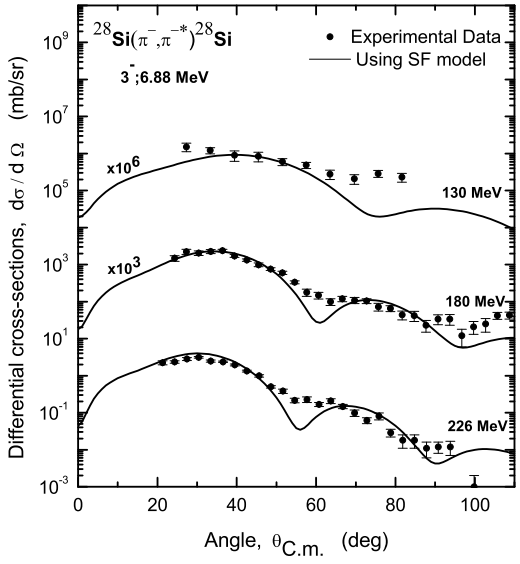

Fig. 9: As in fig.8 but for π^- scattered from ^{28}Si.

Table 6: Deformation parameters β and deformation lengths (δ_{real}, δ_{imag}) from π + ^{28}Si inelastic scattering (2^+;1.78 MeV).

E_{lab} (MeV)	β	δ_{real}	δ_{imag}	β From [15]
π^+				
130	0.42	1.322	1.3266	-
180	0.535	1.7789	1.8601	0.4
226	0.685	1.2792	2.0921	0.37
π^-				
130	0.395	1.6827	1.2022	-
180	0.495	1.6684	1.8404	0.38
226	0.52	1.5952	1.4149	0.35

Table 7: As in table 6 but for π + ^{28} Si inelastic scattering (3^-;6.88 MeV).

E_{lab} (MeV)	β	δ_{real}	δ_{imag}
π^+			
130	0.24	0.7554	0.758
180	0.32	1.064	1.1126
226	0.685	1.2792	2.0921
π^-			
130	0.21	0.8946	0.6391
180	0.29	0.9774	1.0782
226	0.47	1.4418	1.2789

5 Conclusion

[ht] Elastic and inelastic scattering of charged pions from silicon have been analyzed using alpha-clustering single folding model using Dolfin, Hi-Optim and DWUCK4 computers codes. We have obtained a good fit to the experimental data for the elastic scattering of 21.69-226 MeV and the inelastic scattering of 130-226 MeV pions from ^{28}Si. Our results of deformation parameter values with studies estimated by others at 180 and 226 MeV of positive pions confirm the success of our analysis. This success of our analysis on silicon may motivate one to apply this analysis on pions from other nuclei.

References

[1] G. R. Satchler, Nucl. Phys. A540, 533(1992).
[2] L. S. Kisslinger, Phys. Rev. 98,761(1955).
[3] D. F. Jackson, Nuclear Reactions, Science Paperbacks, Chapman and Hall. London, (1975).
[4] M. E. A. Farid and A. A. Ebrahim, Phys. Scr. 90, 015301(2015).
[5] M. E. A. Farid, Z. M. M. Mahmoud and G. S. Hassan, Nucl. Phys. A691, 671-90 (2001).
[6] M. E. A. Farid, Z. M. M. Mahmoud and G. S. Hassan, Phys. Rev. C 64, 014310 (2001).
[7] G. R. Satchler, Nucl. Phys. A540, 533(1992).
[8] L. D. Rickertsen, (unpublished).
[9] N. M. Clarke, Hi-Optim 94.2 Code (1994) (UK: University of Birmingham) unpublished.
[10] E. Friedman et al., Phys. Rev. C72, 034609(2005).

[11] U. Wienands et al., Phys. Rev. C 35, 708 (1987).
[12] B. M. Preedom et al., Nucl. Phys. A326, 385 (1979).
[13] G.R. Satchler, Direct Nuclear Reactions (Oxford University Press, New York, 1983).
[14] P.D. Kunz, computer code DWUCK4, University of Colorado, http://spot.colorado.edu/ kunz/.
[15] V. K. Lukyanov, E. V. Zemlyanaya, K. V. Lukyanov and I. A. M. Abdel-Magead . Analysis of inelastic pion-nucleus scattering within the microscopic optical potential and the in-medium effect on πN amplitude in nuclei. XXII International Baldin Seminar on High Energy Physics Problems, September 15-20, (2014) JINR, Dubna, Russia.